SSRG International Journal of Mechanical Engineering
ISSN: 2348-8360/ https://doi.org/10.14445/23488360/IJME-V13I4P110

Volume 13 Issue 4, 118-131, April 2026

Original Article

Acousto-Ultrasonic Assessment and Machine Learning-Based Defect Classification in Flax Fiber-Reinforced Composites and Natural Flax Fiber-Reinforced Polymer for Sustainable Structures

U Pranavi[1], K. T. Balaram Padal[2]

[1,2]*Department of Mechanical Engineering, Andhra University, Visakhapatnam, Andhra Pradesh, India.*

[1]*Corresponding Author : upranavi908@gmail.com*

Received: 20 January 2026 Revised: 28 February 2026 Accepted: 27 March 2026 Published: 29 April 2026

Abstract- *This paper discusses the concept of Acousto-Ultrasonic Testing (AUT) as a reliable means of measuring the structural integrity of Natural Flax Fiber-Reinforced Polymer (NFRP) composites with non-destructive tests. The Stress Wave Factor was used as the main diagnostic parameter, in which AUT managed to identify and diagnose defects, including voids, delaminations, and microcracks, effectively. Compared to Carbon Fiber-Reinforced Polymer (CFRP) composites, NFRP laminates responded to high damping and variable responses due to the thickness and impact energy; thinner laminates were more effective at absorbing energy but were less stable when exposed to heavy loads. The results of the present study indicate that flax fibers can be used as environmentally friendly alternative materials in composite production. Machine Learning models, such as a Random Forest and Neural Network, have an ideal classification score (F1 score = 1.0), indicating a high degree of fault identification but necessitating more complex datasets to guarantee. This paper contributes to the effectiveness of AUT in sustainable composites and suggests the improvement of signal processing and real-time measurements of smart and environmentally friendly structural applications.*

Keywords *- Flax fiber-Reinforced Polymer (NFRP) composites, Acousto-Ultrasonic Testing (AUT), Machine Learning classification, Non-Destructive Evaluation (NDE), Fault identification and characterisation.*

1. Introduction

Composite materials have experienced wide usage in various engineering industries such as aerospace, automotive, and civil infrastructure, mainly because of their desirable qualities of high strength-to-weight ratio, resistance to corrosion, and design flexibility. Natural fiber-reinforced composites, specifically those made of flax fiber, have become an alternative to traditional synthetic composites in recent years. These materials have great environmental benefits, among them biodegradability, renewability, and a lower carbon footprint, and the competitive mechanical performance is retained. Flax fibers are also used in polymer matrices to increase the load-bearing capacity, which makes them appropriate for structural applications. However, just like other laminated composites, flax fiber-reinforced systems are prone to manufacturing-related defects, including, but not limited to, voids, porosity, delamination, and micro-cracking. These defects may seriously undermine the structural integrity, erode the mechanical performance, and cause early failure in service, unless detected.

In order to overcome these problems, numerous Non-Destructive Testing (NDT) methods have been studied in the literature. A hybrid inspection methodology involving the combination of ultrasonic testing and acoustic tapping to detect internal cavities in stone cultural artifacts was suggested by Wei Qian et al. [1], showing a higher sensitivity to defects in the subsurface without impairing the integrity of the structure. Equally, M. Seleznev et al. [2] used Acoustic Emission (AE) with Ultrasonic Fatigue Testing (USFT) to observe fatigue damage in steel, and found that AE activity during the first loading cycles is a good predictor of micro-crack initiation, with activity rates of 200900 s -1 and signal energy levels of 1100 mV^2. The relevance of NDT techniques was also confirmed by Reddy et al. [3] through the use of rebound hammer testing, ultrasonic pulse velocity, and compressive strength tests to assess the hybrid concrete systems, and the use of NDT in monitoring the evolution of the material property during the curing process was proven.

Improved ultrasonic imaging methods have also been shown to have a great deal of enhancement in defect characterization. The combination of 5 MHz ultrasonic waves with log-Gabor filtering was introduced by X. Yang et al. [4] and demonstrated to provide the ability to reconstruct multilayer CFRP structures in a low signal-to-noise condition. Muflikhun and Fiedler et al. [5] applied acoustic emission and ultrasonic scanning to study crack initiation and propagation in CFRP laminates to test fracture toughness Mode I and the impact of stacking sequence on

fracture behavior. Moreover, Nokhbatolfoghahai and Groves et al. [6] proved that Phased Array Ultrasonic Testing (PAUT) has a better resolution, flexibility, and defect sensitivity than traditional ultrasonic methods when used on composite laminates. Other electromagnetic and hybrid NDT methods have also become popular. Quinn et al. [7] evaluated Ground-Penetrating Radar (GPR) with an antenna of 2000 MHz on thick FRP composites and found that delamination can be detected down to 120 mm depth. Katunin et al. [8] suggested a hybrid approach to experimental NDT data and numerical modeling and Compression After Impact (CAI) testing to assess residual strength in impacted composites. Saeid Hedayatrasa et al. [9] proposed the use of Vibro-Thermal Wave Radar (VTWR), which combines both vibrothermography and coded thermal excitation to achieve deep defects in CFRP structures at low power levels. New high-resolution imaging methods, including Terahertz (THz) and microwave-based NDT, have added to the range of defect detection methods. Zehni et al. [10] used THz spectroscopy, which was upgraded using Multi-Walled Carbon Nanotubes (MWCNTs), to enhance the visibility of damage in GFRP composites with better contrast in comparison to the conventional techniques. Equally, Strom and Swiderski et al. [11] proved that Terahertz imaging (THz) is effective in detecting the presence of subsurface defects like inclusions and air gaps in aramid composites. The study by Omar S. Hassan et al. [12] on microwave NDT to inspect embedded antennas demonstrates an error rate of about 85 percent in detecting defects, as compared to X-ray computed tomography. Moreover, Vishal Balasubramanian et al. [13] proposed an AI-based microwave resonator system with recurrent neural networks to monitor wear depths in real-time with the capability of identifying wear depths up to 2.5 mm.

The latest developments have paid more attention to the incorporation of Artificial Intelligence into NDT methods to enhance the detection and classification of defects. Shaun McKnight et al. [14] proposed a Three-Dimensional Convolutional Neural Network (3D-CNN) model on volumetric ultrasonic data, which has a higher defect detection accuracy at low inference time (under 0.5 s). In another paper, McKnight et al. [15] overcame this shortcoming of a small amount of training data in ultrasonic NDT by introducing four synthetic data generation techniques, using semi-analytical simulations. A modified CycleGAN approach and hybrid simulation-experimental methods among them showed a significant enhancement in the realism of training data over that of purely simulated datasets. Consequently, there was a significant improvement in classification performance with F1 scores reaching 0.843 as compared to 0.394 with traditional simulation-only data. Neha Yadav et al. [16] proposed an inline thermography-based system of inspection of automated tape layup processes, which allows detecting defects in real-time throughout the manufacturing process. Likewise, Meirbek Mussatayev et al. [17] designed a directional eddy current probe for Automated Fiber Placement (AFP), which is able to detect defects, including wrinkles, more than 1.3 mm, with a signal-to-noise ratio of more than 20.

A number of studies have been conducted in the area of natural fiber composites, paying attention to material properties and interfacial behavior. Sunny et al. [18] analyzed the properties and applications of areca nut fiber composites in the development of sustainable products. Madsen et al. [19] examined the impact of porosity on the mechanical performance and established that the higher the porosity, the lower the stiffness and strength of a compound. Yan et al. [20] conducted a review of flax fiber composites and highlighted their structural potential and environmental advantages. George et al. [21] emphasized the importance of fiber-matrix interfacial bonding, but later research showed that interfacial bonding could be enhanced greatly by chemical interventions like alkalization, which would enhance the interfacial adhesion and mechanical performance.

Li et al. investigate the different chemical interventions employed to improve the performance of natural fiber-reinforced composites. Treatments such as alkali, silane, acetylation, and others improve fiber–matrix adhesion by modifying the fiber surface properties. Consequently, these alterations minimize the absorption of moisture and, to a large extent, increase the mechanical properties of the composites [22]. Kabir et al. gives an extensive overview of the surface treatment techniques that are used on natural fibers to improve their compatibility with more advanced composite uses. The different chemical treatments, such as alkali, silane, acetylation, among others, are demonstrated to enhance fiber-matrix bonding, which in turn enhances stress transfer and performance of the composites in general. The treatments have a huge effect on reducing the absorption of moisture and enhancing mechanical strength and dimensional stability relative to untreated fibers [23]. Pickering K.L et al. The studies of natural fiber composites have grown tremendously because of their cheapness and ecological benefits. Fiber properties, processing techniques, and interfacial bonding are some of the factors that determine their mechanical performance. The recent research has shown that their strength and performance are improved, which broadens their engineering uses [24].

Summer scales et al. Plant fibers are inexpensive, renewable reinforcements, although they contain high amounts of hydroxyl, and their surface impurities lower their compatibility with polymer matrices. NaOH alkalization changes their thermal characteristics, crystallinity, and surface morphology, which are measured by DSC, XRD, FTIR, and SEM. These additions enhance the bonding of fibers and matrices, which increases the mechanical and thermal characteristics of the composites [25]. Mwaikambo and Ansell explored the impact of alkalization on hemp, sisal, jute, and kapok fibers, with regard to their thermal, structural, and surface properties. Their experiment showed that sodium hydroxide treatment modifies crystallinity, increases surface roughness, and is more reactive to fibers. These changes enhance fiber-matrix

bonding, leading to an increase in the mechanical and thermal performance of the composites [26]. The article by Azad et al. is a thorough review of intelligent Structural Health Monitoring (SHM) of composite structures, with an emphasis on machine learning, deep learning, and transfer learning methods. The paper has presented the full framework of SHM and its elements, such as sensing technologies, data preprocessing, feature extraction, and decision-making processes in a systematic way. It also identified the contemporary issues and research directions in the future to enhance the reliability and sustainability of composite structures through AI-driven methods [27]. Qing et al. analyzed machine learning-based methods of quantitative damage monitoring of composite structures with a focus on the fact that the old physics-based techniques are limited.

The paper described the combination of sensor networks, data processing, and intelligent algorithms to detect and characterize the damage in an accurate way. It also identified important issues like quality of data, correlation of features, and reliability of the model, and proposed future directions of advanced SHM systems [28]. Hu et al. (2025) suggested a state-of-the-art structural health monitoring system of CFRP structures through the combination of Lamb wave-based NDT and a hybrid CNN Vision Transformer system.

The method involves Continuous Wavelet Transform (CWT) of Lamb wave signals to detect damage automatically and accurately. The findings show enhanced reliability and real-time monitoring, which is not limited by the traditional approaches to managing complicated wave patterns and big data [29]. Amireddy et al. demonstrated the experimental imaging of defects in metallic samples with deep subwavelength ultrasonic images of defects with holey-structured metamaterial lenses, with a resolution of 25 times the wavelength, 25. Geometric parameters were optimised in the study by numerical simulations, and the mechanism was explained by resonant mode coupling and enhanced transmission of waves.

This method enhances the ability to detect defects much better than the traditional ultrasonic resolution limits [30]. Anbalagan et al. (2024) designed a non-destructive testing system based on the use of a rectangular waveguide and a new planar unit cell filter to detect a defect in flax fiber-reinforced composites. The sensor suggested is sensitive to sensing changes in permittivity that are related to defects like voids, cracks, and delamination.

The simulation outcomes have indicated a higher level of defect detection, and this indicates the effectiveness of the microwave NDT in the inspection of natural fiber composite [31]. Saberinaghi et al. examined deep learning-based solutions to detect defects in industrial items and noted that they are better than conventional image processing techniques when dealing with complicated textures, noise, and changing lighting environments. The paper classified the approaches into supervised, semi-supervised, and unsupervised learning and also investigated their use in X-ray image analysis. It also outlined such critical problems as limited data, class imbalance, and real-time processing, and possible ways to enhance the detection performance [32].

Ochoa et al. examined the impact of High-Amplitude Low-Frequency Vibrations (HA-LFV) and machine sound waves on ultrasonic guided wave propagation in composite aircraft structures. It was demonstrated that HA-LFV causes coherent noise as a result of interaction between waves, and this affects signal interpretation to a large degree, whereas audible sound waves do not affect it much. These results are valuable to enhance the dependability of guided wave structural health monitoring during operations [33]. Syed Akbar Ali et al. showed how holey-structured metamaterial lenses could be used to produce deep sub-wavelength ultrasonic imaging with a diffraction limit. The experiment demonstrated that evanescent wave transmission could be used to detect very small defects, including horizontal cracks of scale to 1/25 the wavelength. This method is very useful in ultrasonic NDT to resolve the defects with high precision in characterization [34].

The objective of the current research is to determine the efficacy of Acousto-Ultrasonic Testing (AUT) as a credible non-destructive method of determining the structural integrity of Natural Flax Fiber-Reinforced Polymer (NFRP) composites. It concentrates on the use of the Stress Wave Factor to identify and describe defects like voids, delaminations, and micro-cracks. The paper also examines the dynamic behavior of NFRP laminates compared to CFRP composites under different thicknesses and impact energy levels, which illustrates their damping and stability.

The other important goal is to investigate the potential of NFRP as a more environmentally friendly alternative to the traditional composite materials. Additionally, the work incorporates machine learning methods, such as the Random Forest and Neural Network models, to obtain the correct defect classification with respect to the characteristics of AUT signals, as well as the necessity to use more comprehensive datasets and more advanced signal processing methods to implement structural health monitoring in real-time.

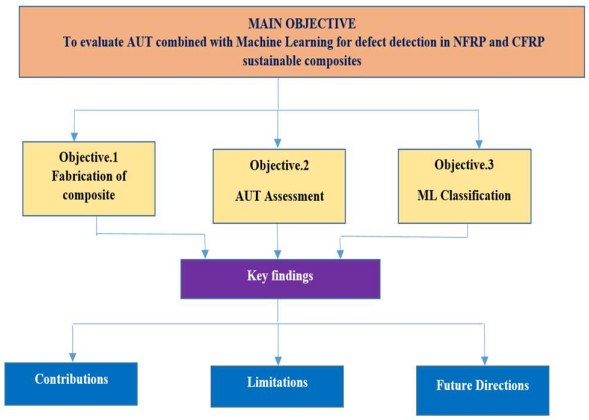

Fig. 1 Schematic outlining of objectives

2. Methodology

The paper employs structured Acousto-Ultrasonic Testing (AUT) in order to determine composite laminates reinforced with carbon fiber and flax natural fiber for fault detection. The three main stages of the technique are data analysis, testing protocols, and composite manufacturing.

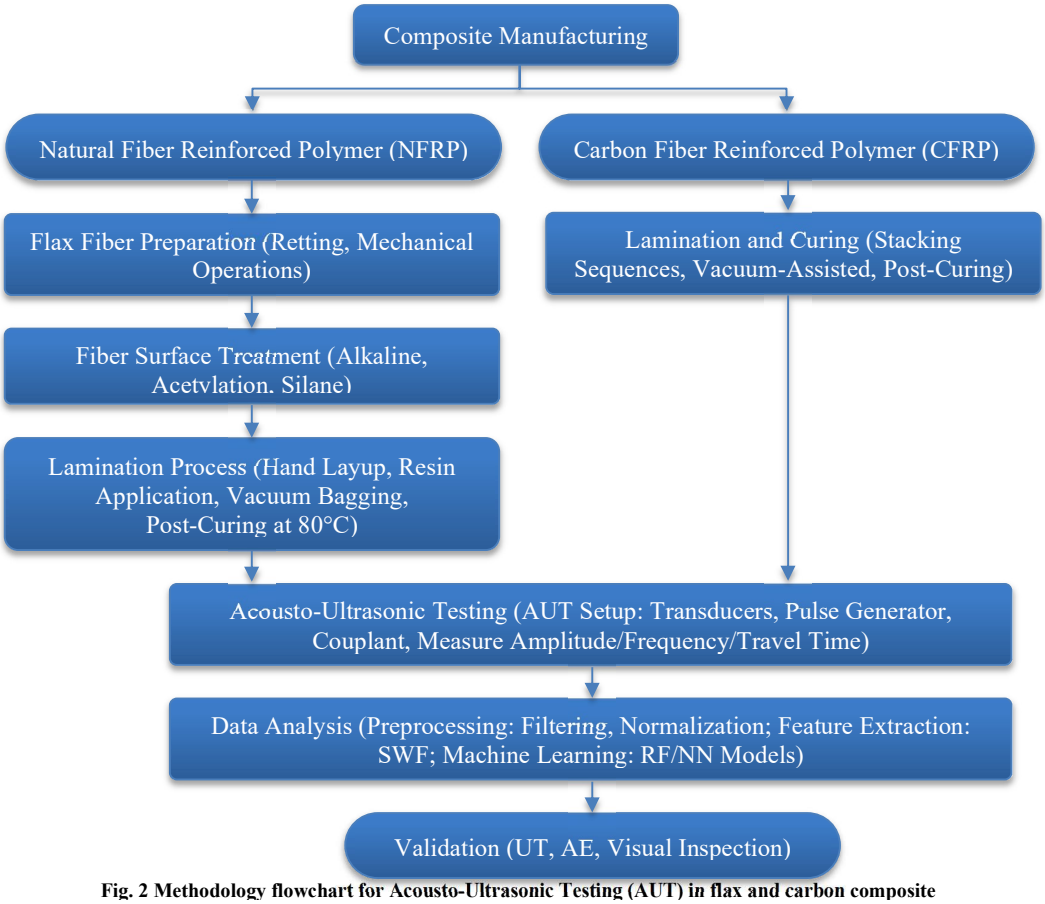

Fig. 2 Methodology flowchart for Acousto-Ultrasonic Testing (AUT) in flax and carbon composite

2.1. Composite Fabrication

2.1.1. Natural Flax Fiber-Reinforced Composites (NFRP)

Flax fiber-reinforced polymer composites were made using an environmentally friendly hand layup technique, which is widely utilized for natural fiber composites due to its versatility and ease of use. Woven flax fibers were chosen for reinforcement because of their beneficial mechanical properties, biodegradability, and renewable nature. Epoxy resin was utilized as the matrix due to its remarkable mechanical strength, high adhesion, and thermal stability. Even though bio-resins might be prospective replacements for future developments, epoxy was selected for this study because of its mechanical performance, stability, and reliability.

2.1.2. Fiber Surface Treatment

The surface of flax fibers was also modified to enhance the interfacial bond between the fiber and the matrix. In alkaline treatment, 5-10% of sodium hydroxide (NaOH) was used to create roughness on the surface, eliminate impurities, and improve adhesion to the matrix. Certain samples were also subjected to extra conditions, e.g., acetylation and silane coupling agents (15-5%) to make them more amenable to the polymer matrix.

2.1.3. Flax Fiber Preparation and Processing

Extraction and preparation of fibers were done systematically before composites were made. Some of the retting methods employed included dew, water, and enzymatic retting to remove the fibers of the flax stems. Mechanical operations like breaking, scutching, and hackling were followed by cleansing and alignment of the fibers.

2.1.4. Lamination Process

Mechanical behavior and structural balance. Anisotropy was achieved by cutting the flax plies to the appropriate size and stacking them together in [0/90] alternating layers. In order to apply resin, it was applied using rollers or brushes. Manual compression was done to eliminate the excess resin and air bubbles. As an alternative, vacuum bagging was used to improve laminate quality and boost consolidation. The composite was then post-cured for two hours at 80°C, which enhanced its mechanical and thermal properties and promoted further cross-linking.

2.2. Carbon Fiber-Reinforced Composites (CFRP)

Because carbon fiber laminates are used in structural and high-performance applications, a similar but more precise procedure was used to make them. Woven or unidirectional carbon fabrics were used, depending on the mechanical requirements.

2.2.1. Lamination and Curing Process

The carbon fiber plies were sliced and arranged in important stacking sequences, such as [0°/90°] or [±45°], to modify the stiffness and strength properties. The layup process included resin impregnation, vacuum-assisted consolidation, ambient curing, and oven post-curing to enhance matrix cross-linking. In order to help identify damage during mechanical testing, artificial defects such as voids and delaminations were intentionally created in a few specimens.

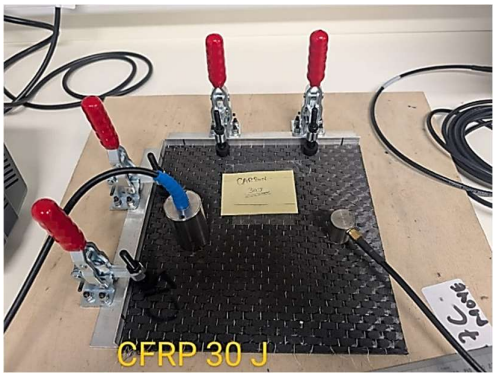

Fig. 3 Carbon fiber reinforced diagram

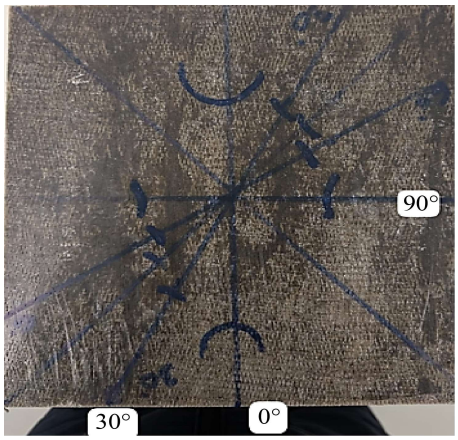

Fig. 4 Illustration of flax fiber in nature

2.2.2. Composite Fabrication Methods with Quality Control and Curing Process

Depending on the kind of matrix material, the composites were made using various manufacturing techniques. In the case of thermoset matrices, such as epoxy and polyester, a hand laydown process with an average fiber volume percentage of 30%–50% was used in conjunction with a vacuum infusion process at a pressure of 0.81 bar. Compression molding was also used to make certain consolidation with the pressure of 2-10 MPa and temperatures of 80°C- 150°C.

On the other hand, thermoplastic matrices like Polylactic Acid (PLA) and Polypropylene (PP) were processed by hot pressing at 180 - 220°C and injection molding at 160 - 220°C. The cooling rates between 2 and 10° C/minute in order to control and retain material integrity and maximize mechanical performance took place during these processes. Depending on the kind of matrix material to be employed in the composite, different curing methods were employed.

The composites (epoxy) were first allowed to cure at room temperature before post-curing under 80°C within two hours to increase the overall mechanical properties and to increase cross-linking within the resin matrix. In contrast, thermoplastic composites require slow cooling after their production. This regulated cooling was necessary to provide dimensional stability and make the mechanical performance of the solidification process predicfig by reducing internal tensions and avoiding warping or distortion.

The manufacturing process was strictly followed in quality control to make sure that the composites are reliable and performance-oriented. To avoid any defects that could compromise the integrity of the structure, the void content was maintained at 5% all times. Also, the balanced distribution of fibers and matrix material was ensured through careful regulation of the volume fraction of the fiber in the optimal range of 30-50 percent to achieve increased mechanical characteristics and composite quality as a whole.

2.3. Acousto-Ultrasonic Testing (AUT)

Following the manufacturing, AUT was used to test interior integrity. It was comprised of piezoelectric transducers, a pulse generator, and an AE win software data collection system. The transducers are mounted on the opposite sides of each specimen with the right couplant to enhance the effective transmission of the waves. At the points where ultrasonic pulses were administered through the material and interacted with faults, amplitude variations, frequency, and travel time were all important pointers to structural anomalies.

2.4. Data Analysis and Validation

Both time-domain and frequency-domain characteristics were used to analyze the collected wave signals to extract Stress Wave Factors (SWF). Such SWFs were plotted across the composite surface with the help of visual aids like the heatmaps in order to identify and define any defective areas. To confirm the findings of the Acousto-Ultrasonic Testing (AUT), cross-checking was done with the traditional Non-Destructive Testing (NDT) methods like Ultrasonic Testing (UT) and Acoustic Emission (AE). These techniques provide additional data on the nature and location of internal defects. There were also visual inspections done to provide precision and uniformity in the total assessment and supplement the geographic mapping of defects. This multiple validation approach enhances the accuracy of the defect diagnosis and characterization process.

The produced flax fiber composites exhibited 60-80% of mechanical properties as compared to traditional glass fiber composites with a 40% density reduction (1.2-1.4 g/cm^3). Due to this fact, they are attractive in terms of application in the automotive, aerospace, and construction industries, where the cost-effective nature, sustainability, and weight minimization are vital.

2.4.1. Testing Parameters and Preprocessing

Preprocessing: To eliminate the high-frequency of the electromagnetic interference and low-frequency mechanical noise, raw AUT signals were filtered using a 4th-order Butterworth bandpass filter with a passband of 50 kHz to 500 kHz. A 50 μs pre-trigger recording was used for baseline noise subtraction. To guarantee uniform feature scaling across all specimens, waveforms were normalized by their maximum amplitude. Feature Extraction: From the processed signals, the essential features for machine learning were taken out.

Stress Wave Factor (SWF): SWF = (Peak Amplitude x Signal Energy) / Signal Duration

2.4.2. Machine Learning Model and Hyperparameter Choices

A Random Forest (RF) and a Neural Network (NN) were the two classifiers used. Grid search was used to determine the ideal configuration for the Random Forest model, which was set as follows: 200 trees, a maximum depth of 10, two samples per leaf, and the "Gini impurity" criterion for node splitting. A feedforward network with an input layer of five features, two hidden layers with 64 and 32 neurons, respectively, and an output layer with a single neuron for binary classification made up the neural network architecture.

The output layer was subjected to the sigmoid function, and the hidden layers were activated by the Rectified Linear Unit (ReLU). Binary cross-entropy was used as the loss function, and the Adam optimizer with a learning rate of 0.001 was used to train the model.

2.4.3. Data Splitting and Validation

A 70% training set and a 30% test set were created from the entire dataset of 270 AUT signal samples, which were gathered from 45 specimens with six measurements each. A stratified split was used to ensure a representative evaluation by maintaining the same proportion of defect classes in both the training and test sets, while a 5-fold cross-validation technique was used on the training set to adjust the hyperparameters and avoid overfitting.

3. Results and Discussion

The results of the study indicate the degree of success of Acousto-Ultrasonic Testing (AUT) to identify and describe internal defects in composite laminates with the help of flax natural fiber. The main objectives of the investigation consisted of finding the locations of the defects, assessing the stress wave propagation through the material, and comparing the outcomes with other Non-Destructive Testing (NDT) methods.

The response of the stress waves in areas of the composite laminates that were identified to be flawless showed obvious evidence of similarity of materials used and the structural integrity. Propagation of the stress waves across these healthy zones was fairly constant, and the key parameters used, like amplitude, Time-of-Flight (ToF), and speed of the wave, were consistent and reproducible.

Such consistency proves the continuity and soundness of the matrix-fiber contact that is a prerequisite of the reliable mechanical performance of the latter and the absence of any internal defects. It was also found that there was minimal attenuation and dispersion of waves in these zones, and this implied that there was a homogeneous inner structure that lacked serious disruptions and material irregularities capable of obstructing the transmission of waves. These findings indicate the efficiency of the material quality in undisturbed regions of laminate architecture and production.

Computations are made to arrive at Stress Wave Factor (SWF) and time-domain parameters in AUT, which are determined using signal characteristics that are due to the interaction of ultrasonic or acoustic waves with the material. These measurements have been proven to be good pointers to the presence of defects not in open sight and in tracking the amount of damage, and give significant information on the structural state of the material.

3.1. Factors in the Time Domain

3.1.1. Rise Time (RT)

This is the period of time taken by the signal between the commencement of the signal and its peak amplitude. It could be helpful in defining the type of damage or material reaction, and shows the speed of accumulation of the stress or acoustic wave. Its description is represented in equation (1).

$$T = \text{Peak time (Tp)} - \text{Start time (Ts)} \quad (1)$$

The overall highest amplitude of the signal is represented by Tp. The starting point, Ts, is beginning to be exceeded.

3.1.2. Decay Time (DT)

The Decay Time (DT) is the duration of time taken between the end of the signal and the peak amplitude. It depicts the rapidity of the signal energy to dissipate in the material, and it is affected by damping properties and internal imperfections. One of its descriptions is given in equation (2).

$$DT = T_E - T_p \quad (2)$$

TE represents the moment of the signal at which the signal takes the value of a constant.

3.1.3. The Length (D)

The Duration (D) is the total time span between the beginning and the end of the signal. It shows the overall propagation and attenuation of the wave within the material

and is susceptible to damage and heterogeneity of the material. One of its depictions is presented in equation (3).

$$D = T_E - T_s \quad (3)$$

3.1.4. Energy (β)

The total energy of the signal is the result of the integration of the square of the signal amplitude over the entire time basis. It gets the intensity of the stress wave or acoustic emission, and greatly depends on the extent of damage and the damping characteristics of the material.

$$E = \int_{T_{start}}^{T_{end}} a(t)^2 dt \quad (4)$$

3.2. Stress Wave Factors

The effect of the stress waves on the material is described by stress wave factors, which are usually determined by both the time and frequency domain data.

3.2.1. Stress Wave Factor (SWF)

It is an index of signal intensity normalized and corrected by the peak amplitude and length of the signal. It is a non-dimensional evaluation of the energy that the stress waves carry.

The metric is specifically effective in acoustic emission or ultrasonic testing to assess the extent of occurrence or damage in materials regardless of certain parameters of the test arrangement.

*S*tress wave factor = β /(D*A)

3.2.2. Frequency Parameters

It has been said that stress wave behaviour can be characterized by frequency content, which gives valuable information about the material reaction and damage processes. The frequency of the signal in which it has the greatest energy (i.e., the frequency that has the largest value) is known as the dominant frequency, and the range of frequencies over which the signal has a significant amount of energy (i.e., wave dispersion, attenuation, and defects in the material) is known as the bandwidth (Δf).

3.2.3. Factor of Attenuation (F_a)

The division of change in amplitude (ΔX) over change in distance (Δx) is called amplitude attenuation (1) and measures the rate at which the signal amplitude decays across the material.

$$Fa = \frac{\Delta X}{\Delta x}$$

The wave velocity (v), which is computed by dividing the distance traveled by the time elapsed ($v = d/t$), reveals the stiffness and integrity of the material. The presence of damage or heterogeneity is often indicated by variations in this value. The properties of materials composed of Natural Fiber Reinforced Polymer (NFRP) and Carbon Fiber Reinforced Polymer (CFRP) are compared in the Domain of Time Table 1. For every material, three duplicate measurements of the time-domain characteristics (amplitude, duration, rise time, and decay time) are made to guarantee repeatability, dependability, etc.

Table 1. Represents the time domain analysis of AUT

Material	The Domain Time Parameters	Property			
		I	II	III	Mean
Carbon Fiber Reinforced Polymer	Time Increase, Sec	1.7E-07	1.7E-07	1.7E-07	1.7E-07
	Time of Decay, Sec	1.5E-07	1.3E-07	1.3E-07	1.23E-07
	The Duration	1.000004	3.7E-06	2.000004	3.83E-06
	The Amplitude	1.102675	1.103844	1.10276	1.10276
Natural Fiber Reinforced Polymer	Time Increase, Sec	1.5E-07	1.6E-07	1.6E-07	1.6E-07
	Time of Decay, Sec	1.7E-06	1.7E-06	1.6E-06	1.83E-06
	The Duration	4.3E-07	1.000006	4.3E-07	5.23E-07
	The Amplitude	1.062622	1.062532	1.053342	1.062635

3.3. Explanation of Parameters

The analysis of signal characteristics reveals important differences between composites made of Natural Fiber-Reinforced Polymer (NFRP) and Carbon Fiber-Reinforced Polymer (CFRP). In all materials, it was found that the rise time, a measurement of how long it takes for the signal amplitude to rise from the mean position to its peak, was consistently fast.

Both values showed consistent behavior across replicates, with an average rise time of 2.6×10^{-2} seconds for CFRP and a slightly faster rise time of 2.4×10^{-1} seconds for NFRP. The average decay time for CFRP was 2.33×10^{-2} seconds, with minimal variation between samples ranging from 2.2×10^{-2} to $2.4 \times 10^{-\circ}$ seconds. The signal's decay time is the amount of time it takes to return to its baseline.

On the other hand, NFRP was found to have a slower signal dissipation, and the decay duration was longer and more stable with an averaged decay of 2.73 x 10^{-1} and a range of 2.6 x 10^{-7} to 2.8 x 10^{-7} seconds. The total signal time (or the entire time taken between the opening and closing) was also a little higher in the case of NFRP, where the average signal time was 5.13 x 10^{-2} vs 4.93 x 10^{-2} in the case of CFRP. Lastly, the amplitude, or the highest value of the signals generated, was greater in CFRP (0.10376) than it was in NFRP (0.072835), indicating that CFRP generated

a stronger signal response. Such variations in signal behavior reflect the natural behavior of the materials, which can play a role in their use in some dynamic or impact-sensitive performance.

3.4. Observation and Interpretations

Significant data on signal intensity, material damping characteristics, and signal uniformity are also given during the analysis of signal characteristics of both the CFRP and NFRP composites. The fact that constantly increasing times were observed in all copies of both materials indicates a strong level of signal consistency and repeatability, which are indicative of a strong material behavior when repeatedly activated. Such reliability is required when the application requires reliable signal delivery or surveillance. Moreover, NFRP is more damping than CFRP; therefore, it can possibly absorb and distribute vibrational energy better due to its longer and more stable decay time.

NFRP is thus a very good option when it comes to applications that need energy dissipation, like vibration damping or noise reduction. On the other hand, CFRP shows a larger signal amplitude and hence indicates a stronger signal response. This implies that CFRP is more effective in terms of reflecting or transferring energy, and it is in line with its application in structural applications where the stiffness and strength of the material are important. These findings show the complementary nature of CFRP and NFRP since CFRP performs well in terms of high-intensity and strength,

3.4.1. Comparison of Materials

Figure 5 shows that the larger amplitude and reduced signal duration of the CFRP make it a stiff yet low-damping material that can be used in high-performance and structural applications. Conversely, NFRP would be more applicable in applications that require mitigating impact or absorbing vibration due to its longer signal, meaning more energy absorption and damping.

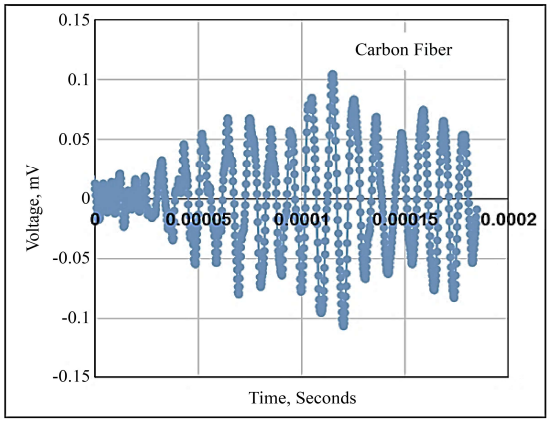

Fig. 5 Represents the Time-Voltage Plot illustrating the AU waveforms of the test

3.4.2. Observations

The characteristics of the damped sinusoidal waveform of the observed signal have a burst of oscillations that decrease in amplitude over time as the energy is dissipated in the material. This is a signal that is linked with carbon-flax composite material, and very likely it was created during a Non-Destructive Test (NDT) procedure like ultrasonic testing, which is normally employed in order to determine the integrity of internal structures. The waveform starts at an approximation of 0 mV and reaches a peak of approximately 0.13 mV at the 0.0001-second point and then exponentially decays, which suggests damping behavior. It is a crucial attribute in structural and acoustic performance studies, as it is a kind of decay that exhibits the way in which the material takes in and gives back the vibrational energy. The overall signal time is approximately 0.0002 seconds (200 microseconds), in line with the ultrasonic echo time in composite materials.

The waveform may be part of an ultrasonic backscatter or through-transmission signal in order to detect internal flaws or material heterogeneity in carbon flax composites. The acoustic-ultrasonic waveforms captured during the test are shown in the image, along with how the Time-Voltage Plot illustrates changes in signal amplitude over time: polymers reinforced by natural fibers having an impact energy of 10J.

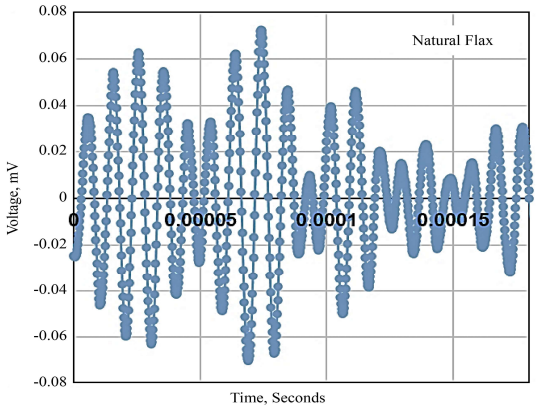

Fig. 6 Represents how the amplitude fluctuates for NFRP

The picture shows a temporal domain analysis of recorded ultrasonic waves during many test strikes. Four polymers reinforced with carbon fiber at a 20J impact energy were used to demonstrate how the signal's amplitude varies over time.

The stress wave characteristics under various impact energy and thickness conditions are displayed in Table 2 for two distinct materials (CFRP and NFRP). The energy, peak voltage, and ring-down time are calculated once the impact energy is assessed for the given materials.

The confusion matrix indicates that the model performed rather well in recognizing the supplied data. It shows that all four samples in class 1 and all eleven samples in class 0 were properly predicted to be class 1 and class 0, respectively. Importantly, no misclassifications occurred since there were neither false positives nor false negatives. This suggests that the model has effectively distinguished between the two groups.

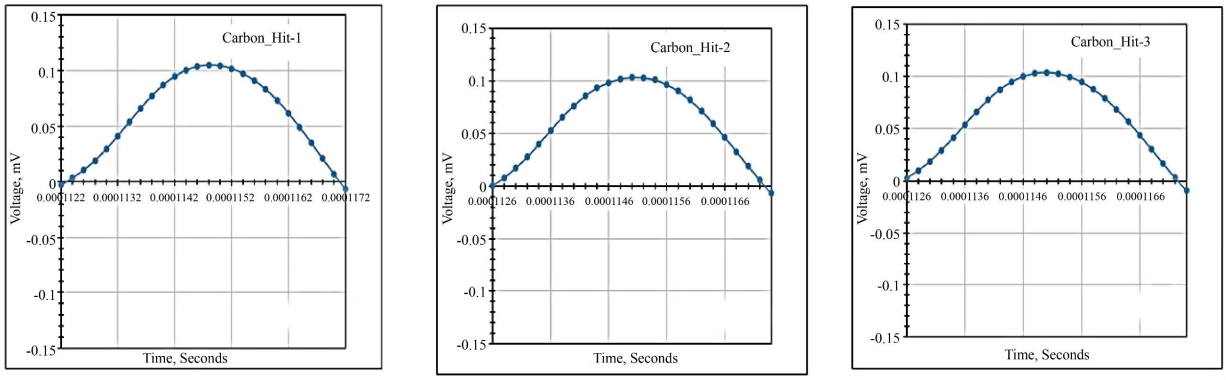

(a) (b) (c)

Fig. 7 Time-domain analysis of ultrasonic signals obtained from (a) Hit number 1, (b) Hit number 2, and (c) Hit number 3 revealed waveform features and amplitude fluctuations.

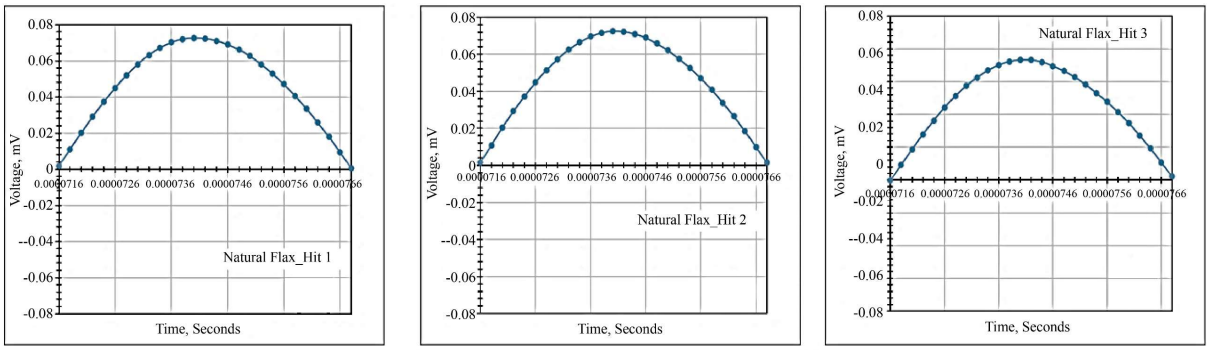

(a) (b) (c)

Fig. 8 Depicts the waveform features and amplitude fluctuations for hits (a), (b), and (c) 1, 2, and 3

Table. 2 Determining the factors of stress waves

Materials	Thickness mm	Impact Energy (J)	Factor of Stress Wave		
			Maximum Voltage-mV	Ring Down, Sec.	The Energy
Carbon Fiber Reinforced Polymer	1.4 mm	20J	102.7	1.3E-06	89
	1.4 mm	10J	44.13	1.33E-06	25
	1.5 mm	20J	212.5	1.4E-06	116
Natural Fiber Reinforced Polymer	4 mm	20J	72	3.73E-06	32
	2 mm	10J	134.8	1.8E-06	200
	4 mm	20J	22.14	3.6E-06	10

Table 3. Using statistical stress wave parameters to calculate signal noise ratio levels

Materials	Thickness mm	Impact Energy (J)	SWF			SN-L
			(Y1-The Peak Voltage mV)	(Y2- Ring Down, sec)	(Y3- Energy, J)	
1. Carbon Fiber Reinforced Polymer	1.5	20	104.8	1.20E-06	89	-18.0346
	3.40	30	44.09	4.33E-06	29	-13.7481
	3.40	20	212.5	3.40E-06	112	-20.3543
2. Natural Fiber Reinforced Polymer	4 .00	20	72	1.73E-06	32	-15.3991
	4 .00	30	134.8	4.80E-06	117	-19.2393
	2 .00	20	22.14	3.60E-06	02	-7.25928

Table 4. Comparison of the present study results with the literature on NDT and ML for composite defect classification

Reference	Material	NDT Technique	ML Approach	Key Findings
Present Study	NFRP (Flax) & CFRP	Acousto-Ultrasonic Testing (AUT)	Random Forest, Neural Network	AUT with Stress Wave Factor (SWF) effectively identified voids, delamination, microcracks; NFRP showed higher damping; CFRP showed higher energy transmission; ML achieved perfect classification
Zhang et al. [29]	Flax composites	Ultrasonic imaging	CNN	Classified flax composite ultrasonic images with high accuracy despite material anisotropy
Almeida et al. [30]	Flax laminates	Acoustic Emission (AE)	Not applied	Linked AE characteristics to specific damage types under flexural loading
Hossain et al. [31]	Jute & flax hybrid composites	Terahertz imaging	Not applied	Identified subsurface defects in non-conductive composites
Nguyen et al. [32]	Composite laminates	Ultrasonic + Thermal	Hybrid deep learning	Multi-defect classification improved by fusing multimodal NDT data

3.5. Signal--Noise Ratio

Statistical measure of the accuracy of a signal-to-noise ratio.

$$SN - L = -10 \times \log_{10}$$

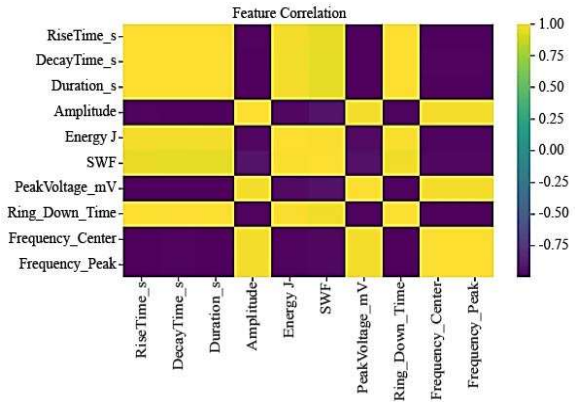

Fig. 9 Feature correlation

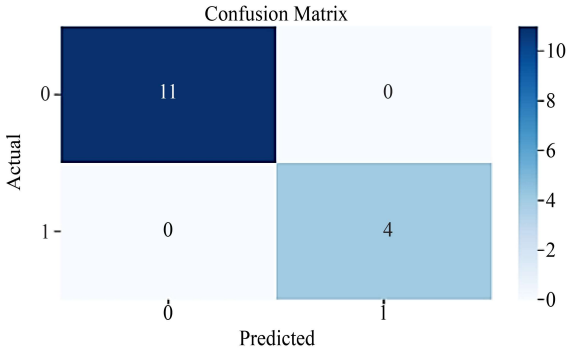

Fig. 10 Confusion matrix

The above findings can be concluded to mean that the model was accurate by 100 percent since all the predictions were correct. Moreover, the accuracy and recall of both classes are 100, meaning that the model not only makes accurate predictions but also removes unnecessary errors. Also, the F1 score, which is the mean of memory and accuracy, is 100, indicating that the person has scored perfectly in all the significant evaluation measures.

Considering the small scale or the simplicity of the dataset, such an ideal performance can indicate that the model can have perfect classification. This is an awesome result, but it also highlights the importance of testing with larger and more varied datasets to be sure that the model is not simply overfitting the small amount of data. The model has, however, proved to be very reliable and effective in the set of tests that had been assigned.

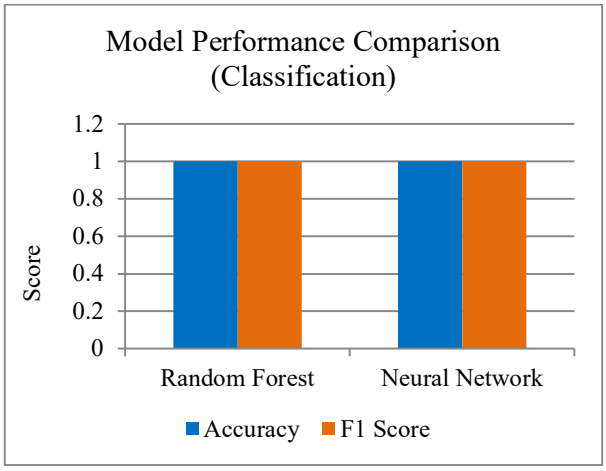

Fig. 11 Comparison of random forest and neural networks algorithms

The bar graph tells the level of classification of data by the random forest and Neural Network models. The two models yielded the same results when the accuracy and F1 scores were at the highest possible value of 1.0. This shows that every model had the ability to perfectly and correctly classify each sample.

The accuracy and the F1 score of the Random Forest model of 1.0 demonstrate that it perfectly balanced the accuracy and the recall, besides being successful in predicting all classes. This performance was also equal to the Neural Network model, which indicated that it is no more effective in detecting the underlying patterns in the data. As both models scored perfectly, there is no significant difference between the classification performance of the models on this dataset. This can indicate that the dataset is either too simple or too simple to provide the models with a challenge. Although the results may be excellent, additional testing on larger and more diverse data would have to be done to determine the effectiveness of these models on larger data. The models got an Area Under the Curve (AUC) of 1.0 on the test set, which means they could tell the difference between defect and non-defect classes perfectly.

3.5.1. Confusion Matrices

Figure 10 demonstrates the confusion matrix based on the performance of the classification models. All four faulty samples were correctly predicted as Class 1, and every one of the 11 good samples landed in Class 0, with no mistakes either way. This led to perfect scores of 100% across accuracy, precision, recall, and F1 for both categories, proving how well the AUT features separate defects in this setup.

3.6. Performance Evaluation using Confusion Matrix, ROC Curve, and Statistical Analysis

The strength of the machine learning models to be used in defect classification and the scientific reliability of the models were imperative; therefore, an all-encompassing evaluation scheme was embraced. These are confusion matrix analysis, Receiver Operating Characteristic (ROC) curve analysis, and statistical validation measures.

3.6.1. Confusion Matrix Analysis

In binary classification, a confusion matrix is used to decompose predictions into four categories. True Positives (TP) are those defective samples that are rightfully reported as defective. True Negatives (TN) are non-defective samples that are rightly identified as not defective. False Positives (FP) are cases when defective samples are mistakenly profiled as non-defective.

False Negatives (FN) occur when flawed samples are incorrectly identified as non-flawed. The model performed correctly, identifying TP = 4, TN = 11, FP = 0, FN = 0. Using these values, the performance metrics are computed as:

Accuracy = (TP + TN) / (TP + TN + FP + FN) = 1.0
Precision = TP / (TP + FP) = 1.0
Recall (Sensitivity) = TP / (TP + FN) = 1.0
F1-Score = 2 × (Precision × Recall) / (Precision + Recall) = 1.0

The confusion Matrix is given by $\mathbf{C} = \begin{bmatrix} 11 & 0 \\ 0 & 11 \end{bmatrix}$

However, such ideal performance must be interpreted cautiously, as it may indicate high feature separability, or Possible overfitting due to limited dataset size.

3.6.2. Receiver Operating Characteristic (ROC) Curve

The ROC curve measures the capacity of the classification model to differentiate between classes with regard to varying threshold values. It is plotted between the True Positive rate

$$TPR = TP/(TP + FN)$$

and for the False Positive rate

$$FPR = FP/(FP + TN)$$

then the values obtained will be TPR = 1.0 and FPR = 0.0.This causes a ROC curve to run through the top-left corner, which reflects perfect classification. The Area Under the Curve (AUC) is given as AUC = 1.0. An AUC = 1.0 corresponds to the Perfect separability of defective and non-defective classes.

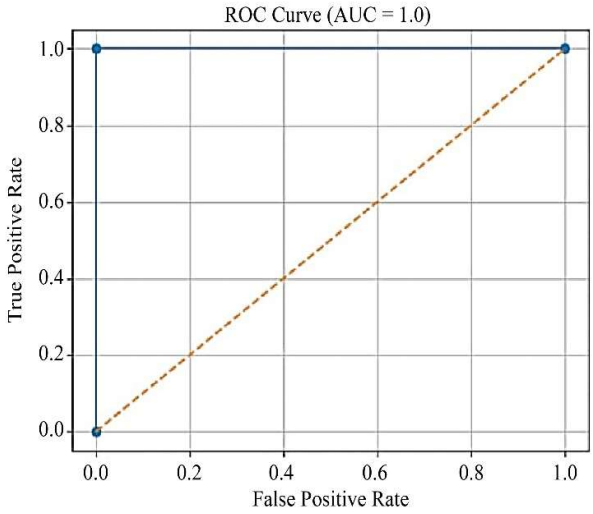

Fig. 12 Representing the ROC curve

Figure 12, ROC curve of the classification performance, where Area under the Curve (AUC) is 1.0, which means that the performance is well separable between the defective and non-defective classes. It is considered that the controlled dataset and the highly discriminative AUT features create the optimum ROC performance, but additional testing on real-world noisy datasets is required.

3.6.3. Statistical Significance Testing

Using the Random Forest and Neural Network models, the predictions on the test data were compared. Random Forest and Neural Network models were compared using.
McNemar Test: To determine their classification performance.

Null Hypothesis (H 0): The performance of both models and the p-value of the null hypothesis are equal. It means that there is no statistically significant difference between the two models, and both models work the same with this data.

Cohen's Kappa Coefficient

The Kappa by Cohen is used to assess the level of agreement between the predicted and actual classification, and it takes into account the agreement due to chance.

Kappa (κ) = 1.0 then

K = 1 implies Perfect agreement, and Confirms model predictions are very reliable.

3.6.4. Signal-to-Noise Ratio (SNR) Validation

Signal-to-Noise Ratio (SNR) was calculated to guarantee the quality of data:

$$SNR = -10 \log_{10} (\text{noise variance/signal variance})$$

Strong signal integrity and Reliable feature extraction are indicated by higher SNR values. The measured SNR values indicate that the signals of AUT are clean at that point, and noise is not a serious issue with classification.

3.7. Discussion on Overfitting and Dataset Limitations

Despite the fact that the models reached an absolute performance (Accuracy = 1.0 and AUC = 1.0), it is possible to explain this by the fact that the data size (270 samples) was small, the conditions of the experiment were controlled, and the features of the defects were easily distinguishable. The possible dangers that these factors bring include overfitting to experimental data and decreased extrapolation to real-life defect situations. To reduce their effects, stratified sampling was used to ensure the balance of classes, and k-fold cross-validation was used to estimate the robustness of the models. Nevertheless, this has to be validated further; additional research is required in the future to involve larger data sets, to work with real-world defect conditions, and to test under noisy and complex signal conditions to make sure it is practically applicable. The data is 270 samples that were obtained by controlled acousto-ultrasonic experiments of composite specimens under different defect conditions. The data used has several defect sizes, defect types, and locations to represent variability in structural response. The acquisition of signals was done with similar loading factors and boundary conditions in order to realize repeatability, and the extraction of the features considered the wave propagation properties. This organized data has a good foundation for model development and validation.

4. Conclusion

The article shows that Acousto-Ultrasonic Testing (AUT) is an effective non-destructive evaluation method of Natural Flax Fiber-Reinforced Polymer (NFRP) composites. The Stress Wave Factor was used by AUT to trace specific defects inaccurately, like voids, delamination, and microcracks, indicating that it can be applied to manufactured and natural composites. Relative analysis indicated that NFRP laminates were more damaged and more sensitive to the energy of impact as well as the breadth than Carbon Fiber-Reinforced Polymer (CFRP) composite, which possesses a greater energy transmission capacity. These results show that designs of custom laminates that achieve a balance between mechanical performance and sustainability are needed.

Even though machine learning classifiers, like the Random Forest and the Neural Networks, demonstrated a high quality of classification (F1 score = 1.0), it is advisable to perform further validation on more diverse data to ensure generalization because of the simplicity of the data. Future studies should focus on complex signal processing and real-time monitoring to come up with intelligent and sustainable composite structures.

The implication of the application of AUT with embedded sensor technologies can provide continuous structural health monitoring of the practiced environmentally friendly composites as well. The next generation of sustainable engineering materials would be enhanced with the use of AUT by adding hybrid systems of composite materials and extending the range of experimentation.

4.1. Study Limitations and Future Research Directions

Though this evidence confirms the efficiency of Acousto-Ultrasonic Testing (AUT) with machine learning to identify the defects of Natural Flax Fiber-Reinforced Polymer (NFRP) composites, the presence of numerous limitations can be noted, and it indicates that many potential research areas can be conducted in the future.

4.2. Limitations of the Present Study

4.2.1. Controlled Defect Introduction

This cannot be adequately replicated in the complexity, structure, and distribution of the naturally occurring defects in the composites made in an industrial setting and subjected to the real-life service loads, but this is natural when carrying out process validation.

4.2.2. Dataset Scale and Complexity

This is an encouraging development, which is probably due to the fact that it is achieving a 100 percent (F1 score = 1.0) on the category of perfectly categorizing data due to the small-scale and controlled experimental dataset.

4.2.3. Material and Processing Variability

The experiment was primarily concentrating on the artificial fiber volume fractions, one of the main epoxy matrices, and a few lamination designs, weave patterns, matrix systems (bio-resins), and production techniques (Automated method), environmental conditioning and many more may influence AUT and the performance of the trained models.

4.3. Recommendations for Future Research

To overcome these limitations and further the field, the following directions of the studies are suggested:

- Future studies should evaluate AUT and ML models on composites with actual manufacturing flaws (such as resin-rich/poor patches and fiber waviness) and in-service damage (like fatigue fractures and barely perceptible impact damage). For samples that are examined in the field, industry collaboration is crucial.
- Field-tested samples require cooperation in the industry. Construction of Large Benchmark Data sets: Large, freely available, fully annotated material sets of AUT/ultrasonic signals of composite buildings with various flaws that are reported should be constructed. This will make ML models well-trained, benchmarked, and generalized.

Ethical Considerations

Not applicable

Acknowledgments

All authors contributed equally to this work.

References

[1] Wei Qian et al., "Improving Non-destructive Testing Methods for Detecting Cavity Damage and Internal Defects in Stone Cultural Relics: A Focus on Ultrasonic Testing and Acoustic Tapping Technology," *Journal of Cultural Heritage*, vol. 67, pp. 479-487, 2024. [CrossRef] [Google Scholar] [Publisher Link]

[2] M. Seleznev, A. Weidner, and H. Biermann, "Detection of Early Fatigue Damage during Ultrasonic Fatigue Testing of Steel by Acoustic Emission Monitoring," *International Journal of Fatigue*, vol. 185, pp. 1-12, 2024. [CrossRef] [Google Scholar] [Publisher Link]

[3] G. Gautham Kishore Reddy et al., "Experimental Studies on Behavior of Hybrid Materials Concrete using Non-Destructive Testing (NDT) Methods," *Materials Today: Proceedings*, pp. 1-6, 2023. [CrossRef] [Google Scholar] [Publisher Link]

[4] Xiaoyu Yang et al., "Comparative Study of Ultrasonic Techniques for Reconstructing the Multilayer Structure of Composites," *NDT & E International*, vol. 121, 2021. [CrossRef] [Google Scholar] [Publisher Link]

[5] Muhammad Akhsin Muflikhun, and Bodo Fiedler, "Comprehensive Evaluation of CFRP Laminates using NDT Methods for Aircraft Applications," *Journal of Materials Research and Technology*, vol. 32, pp. 395-409, 2024. [CrossRef] [Google Scholar] [Publisher Link]

[6] Ali Nokhbatolfoghahai, and Roger M. Groves, *6 - Integrity Assessment of Impacted Thick Composite Laminates using Phased Array Ultrasonic Testing*, Non-destructive Testing of Impact Damage in Fiber-Reinforced Polymer Composites, Woodhead Publishing, pp. 151-185, 2024. [CrossRef] [Google Scholar] [Publisher Link]

[7] James A. Quinn et al., "Novel Application of Ground Penetrating Radar for Damage Detection in thick FRP Composites," *Composites Part B: Engineering*, vol. 284, pp. 1-15, 2024. [CrossRef] [Google Scholar] [Publisher Link]

[8] Andrzej Katunin et al., "Methodology of Residual Strength Prediction of Composite Structures with Low-velocity Impact Damage based on NDT Inspections and Numerical-experimental CAI Testing," *International Journal of Impact Engineering*, vol. 181, pp. 1-21, 2023. [CrossRef] [Google Scholar] [Publisher Link]

[9] Saeid Hedayatrasa et al., "Vibro-Thermal Wave Radar: Application of Barker Coded Amplitude Modulation for Enhanced Low-Power Vibrothermographic Inspection of Composites," *Materials*, vol. 14, no. 9, pp. 1-15, 2021. [CrossRef] [Google Scholar] [Publisher Link]

[10] Ozan Can Zehni et al., "Carbon Contrast Agents for Terahertz Spectroscopic NDT of Impacted Glass Fibre Reinforced Plastics," *Composites Science and Technology*, vol. 257, pp. 1-9, 2024. [CrossRef] [Google Scholar] [Publisher Link]

[11] Martyna Strąg, and Waldemar Świderski, "Non-destructive Inspection of Military-designated Composite Materials with the use of Terahertz Imaging," *Composite Structures*, vol. 306, 2023. [CrossRef] [Google Scholar] [Publisher Link]

[12] Omar S. Hassan et al., "Inspection of Antennas Embedded in Smart Composite Structures using Microwave NDT Methods and X-ray Computed Tomography," *Measurement*, vol. 226, 2024. [CrossRef] [Google Scholar] [Publisher Link]

[13] Vishal Balasubramanian et al., "Non-destructive Erosive Wear Monitoring of Multi-layer Coatings using AI-enabled Differential Split Ring Resonator based System," *Nature Communications*, vol. 14, pp. 1-12, 2023. [CrossRef] [Google Scholar] [Publisher Link]

[14] Shaun McKnight et al., "Three-Dimensional Residual Neural Architecture Search for Ultrasonic Defect Detection," *IEEE Transactions on Ultrasonics, Ferroelectrics, and Frequency Control*, vol. 71, no. 3, pp. 423-436, 2024. [CrossRef] [Google Scholar] [Publisher Link]

[15] Shaun McKnight et al., "A Comparison of Methods for Generating Synthetic Training Data for Domain Adaption of Deep Learning Models in Ultrasonic Non-Destructive Evaluation," *NDT & E International*, vol. 141, pp. 1-14, 2024. [CrossRef] [Google Scholar] [Publisher Link]

[16] Neha Yadav et al., "In-line and Off-line NDT Defect Monitoring for Thermoplastic Automated tape Layup," *NDT & E International*, vol. 137, pp. 1-8, 2023. [CrossRef] [Google Scholar] [Publisher Link]

[17] Meirbek Mussatayev et al., "Directional Eddy Current Probe Configuration for in-line Detection of Out-of-plane Wrinkles," *Composites Part B: Engineering*, vol. 268, pp. 1-13, 2024. [CrossRef] [Google Scholar] [Publisher Link]

[18] Georgy Sunny, and T. Palani Rajan, "Review on Areca Nut Fiber and its Implementation in Sustainable Products Development," *Journal of Natural Fibers*, vol. 19, no. 12, pp. 4747-4760, 2022. [CrossRef] [Google Scholar] [Publisher Link]

[19] Bo Madsen, and Hans Lilholt, "Physical and Mechanical Properties of Unidirectional Plant Fibre Composites—an Evaluation of the Influence of Porosity," *Composites Science and Technology*, vol. 63, no. 9, pp. 1265-1272, 2003. [CrossRef] [Google Scholar] [Publisher Link]

[20] Libo Yan, Nawawi Chouw, and Krishnan Jayaraman, "Flax Fibre and its Composites – A Review," *Composites Part B: Engineering*, vol. 56, pp. 296-317, 2014. [CrossRef] [Google Scholar] [Publisher Link]

[21] Jayamol George, M.S. Sreekala, and Sabu Thomas, "A Review on Interface Modification and Characterization of Natural Fiber Reinforced Plastic Composites," *Polymer Engineering & Science*, vol. 41, no. 9, pp. 1471-1485, 2001. [CrossRef] [Google Scholar] [Publisher Link]

[22] Xue Li, Lope G. Tabil, and Satyanarayan Panigrahi, "Chemical Treatments of Natural Fiber for Use in Natural Fiber-Reinforced Composites: A Review," *Journal of Polymers and the Environment*, vol. 15, pp. 25-33, 2007. [CrossRef] [Google Scholar] [Publisher Link]

[23] M.M. Kabir et al., "Chemical Treatments on Plant-based Natural Fibre Reinforced Polymer Composites: An Overview," *Composites Part B: Engineering*, vol. 43, no. 7, pp. 2883-2892, 2012. [CrossRef] [Google Scholar] [Publisher Link]

[24] K.L. Pickering, M.G. Aruan Efendy, and T.M. Le, "A Review of Recent Developments in Natural Fibre Composites and their Mechanical Performance," *Composites Part A: Applied Science and Manufacturing*, vol. 83, pp. 98-112, 2016. [CrossRef] [Google Scholar] [Publisher Link]

[25] John Summerscales et al., "A Review of Bast Fibres and Their Composites. Part 1 – Fibres as Reinforcements," *Composites Part A: Applied Science and Manufacturing*, vol. 41, no. 10, pp. 1329-1335, 2010. [CrossRef] [Google Scholar] [Publisher Link]

[26] Leonard Y. Mwaikambo, and Martin P. Ansell, "Chemical Modification of Hemp, Sisal, Jute, and Kapok Fibers by Alkalization," *Journal of Applied Polymer Science*, vol. 84, no. 12, pp. 2222-2234, 2002. [CrossRef] [Google Scholar] [Publisher Link]

[27] Muhammad Muzammil Azad et al., "Intelligent Structural Health Monitoring of Composite Structures using Machine Learning, Deep Learning, and Transfer Learning: A Review," *Advanced Composite Materials*, vol. 33, no. 2, pp. 162-188, 2024. [CrossRef] [Google Scholar] [Publisher Link]

[28] Xinlin Qing et al., "Machine Learning Based Quantitative Damage Monitoring of Composite Structure," *International Journal of Smart and Nano Materials*, vol. 13, no. 2, pp. 167-202, 2022. [CrossRef] [Google Scholar] [Publisher Link]

[29] Huanjia Hu, Xuebin Xu, and Cheng Liu, "Structural Health Monitoring of CFRP Composite Structures Using a Hybrid CNN-Vision Transformer Model," *2025 International Conference on Sensing, Measurement & Data Analytics in the era of Artificial Intelligence (ICSMD)*, Guangzhou, China, pp. 1-6, 2025. [CrossRef] [Google Scholar] [Publisher Link]

[30] Kiran Kumar Amireddy, Krishnan Balasubramaniam, and Prabhu Rajagopal, "Deep Subwavelength Ultrasonic Imaging using Optimized Holey Structured Metamaterials," *Scientific Reports*, vol. 7, pp. 1-8, 2017. [CrossRef] [Google Scholar] [Publisher Link]

[31] Arunkumar Anbalagan et al., "A Novel Microwave-based Non-destructive Testing System for Detection of Sub-surface Defects in Natural Flax Fiber Reinforced Composite Material," *Proceedings of the Institution of Mechanical Engineers*, *Part L: Journal of Materials: Design and Applications*, vol. 238, no. 4, pp. 693-706, 2024. [CrossRef] [Google Scholar] [Publisher Link]

[32] Alireza Saberironaghi, Jing Ren, and Moustafa El-Gindy, "Defect Detection Methods for Industrial Products Using Deep Learning Techniques: A Review," *Algorithms*, vol. 16, no. 2, pp. 1-30, 2023. [CrossRef] [Google Scholar] [Publisher Link]

[33] Pedro A. Ochôa, Roger M. Groves, and Rinze Benedictus, "Effects of High-amplitude Low-frequency Structural Vibrations and Machinery Sound Waves on Ultrasonic Guided Wave Propagation for Health Monitoring of Composite Aircraft Primary Structures," *Journal of Sound and Vibration*, vol. 475, pp. 1-21, 2020. [CrossRef] [Google Scholar] [Publisher Link]

[34] Mohamed Subair Syed Akbar Ali et al., "Characterization of Deep Sub-wavelength Sized Horizontal Cracks Using Holey-Structured Metamaterials," *Transactions of the Indian Institute of Metals*, vol. 72, pp. 2917-2921, 2019. [CrossRef] [Google Scholar] [Publisher Link]